Hydrodynamic excitations in a spin-polarized Fermi gas under harmonic confinement in one dimension

A. Minguzzi, P. Vignolo, M. L. Chiofalo, and M. P. Tosi

Istituto Nazionale per la Fisica della Materia and Classe di Scienze, Scuola Normale Superiore, Piazza dei Cavalieri 7, 56126 Pisa, Italy

We consider a time-dependent nonlinear Schrödinger equation in one dimension (1D) with a fifth-order interaction term and external harmonic confinement, as a model for both (i) a Bose gas with hard-core contact interactions in the local-density approximation, and (ii) a spin-polarized Fermi gas in the collisional regime. We evaluate analytically in the Thomas-Fermi limit the density fluctuation profiles and the collective excitation frequencies, and compare the results for the low-lying modes with those obtained from numerical solution of the Schrödinger equation. We find that the excitation frequencies are multiples of the harmonic-trap frequency even in the strong-coupling Thomas-Fermi regime. This result shows that the hydrodynamic and the collisionless collective spectra coincide in the harmonically confined 1D Fermi gas, as they do for sound waves in its homogeneous analog. It also shows that in this case the local-density theory reproduces the exact collective spectrum of the hard-core Bose gas under harmonic confinement.

I. INTRODUCTION

The study of atomic gases in condensed quantum states inside magnetic or optical traps has received an enormous impulse from the achievement of Bose-Einstein condensation in vapors of bosonic alkali-metal atoms and of atomic hydrogen [1]. Similar techniques of trapping and cooling are being used to bring gases of fermionic alkali-metal atoms into the quantum degeneracy regime [2]. The observation of small-amplitude shape-deformation modes in Bose-Einstein condensates inside three-dimensional (3D) anisotropic traps at extremely low temperatures [3] has proved to be an important method of diagnostics and has provided a crucial test of the mean-field theory based on the time-dependent Gross-Pitaevskii equation [4]. No such experiments have as yet been observed in Fermi gases, but predictions are available for their dynamical spectra in both the collisional and the collisionless regime [5]. For both bosons and fermions in 3D the strong-coupling Thomas-Fermi limit is characterized by a different spectrum from the weak-coupling limit.

Attention has also been moving toward atomic gases in restricted geometries, where new frontiers are met in the realization of atom lasers [6,7] and of thin atom waveguides [8]. The rich phase diagram of a quasi-1D Bose gas may become accessible to observation through tuning of the interactions [9]. Essential modifications to the Gross-Pitaevskii equation are needed in $D \leq 2$, since the T matrix already vanishes in $D=2$. The dilute gas limit can still imply strong coupling in 1D, since collisions are unavoidable in this reduced dimensionality.

At low temperature and density the dynamics of a Bose gas with repulsive interactions inside a very thin waveguide approaches that of a 1D fluid of impenetrable pointlike bosons [8]. As demonstrated by Girardeau [10], this so-called Tonks gas [11] has the same spatial profiles as those of a spin-polarized Fermi gas, since the exact many-boson wave function is related to that of noninteracting spinless fermions by $\Psi_B(x_1, \ldots, x_N) = |\Psi_F(x_1, \ldots, x_N)|$. More generally, the

Fermi-Bose mapping theorem implies that the dynamic structure factor of the Tonks gas is the same as that of the corresponding ideal Fermi gas, although their momentum distributions are very different. In particular, in the same work Girardeau [10] also showed that long-wavelength sound waves propagate in the homogeneous Tonks gas with velocity $v = \pi \hbar n/m$ equal to the Fermi velocity v_F in the homogeneous ideal Fermi gas at the same density n and atom mass m. This is, in fact, the speed of propagation for both zero (collisionless) sound and hydrodynamic sound in the ideal 1D Fermi gas.

The dynamic structure factor of the spin-polarized 1D Fermi gas under harmonic confinement has been evaluated exactly in the collisionless regime and related to that of the homogeneous gas by means of a local-density formula [12]. The collective excitation frequencies in this regime are integer multiples of the harmonic-trap frequency and this spectrum is, therefore, also that of the corresponding Tonks gas. In the present work we evaluate the dynamics of the same Fermi system in the collisional regime described by linearized hydrodynamic equations. We show how these equations for the Fermi gas can be derived from the nonlinear Schrödinger equation proposed by Kolomeisky *et al.* [13] for the dynamics of the mesoscopic wave function of the corresponding Tonks gas and how the equality of the spectra of the two fluids remains valid within the dynamical regime of present interest.

After a presentation of the model in Sec. II, we evaluate its dynamical density fluctuations and collective frequency spectrum in the following sections. We give in Sec. III an analytical solution of the equations of motion for the density fluctuations, using the Thomas-Fermi approximation (TFA), extended, however, to consider solutions external to the classical radius. In Sec. IV we treat the same problem by means of a numerical simulation mimicking an experimentally realizable method for measuring the frequencies of the gas. That is, we excite a collective mode of the atomic cloud by applying an external time-dependent potential of chosen symmetry and probe it by observing the evolution in time of the

density profile once the perturbation is turned off. Finally, Sec. V gives a brief summary of our main results and some concluding remarks.

II. THE MODEL

According to Kolomeisky *et al.* [13], a long-wavelength approach to the hard-core 1D Bose gas with repulsive point-like interactions in the dilute regime can be based on the nonlinear Schrödinger equation

$$i\hbar\partial_t\Phi(x,t) = \left[-\frac{\hbar^2}{2m}\partial_x^2 + V(x,t) + \frac{\pi^2\hbar^2}{2m}|\Phi(x,t)|^4\right]\Phi(x,t). \quad (1)$$

Here, $V(x,t) = V_{ext}(x) + U_p(x,t)$ is a time-dependent external potential, which includes the harmonic confinement $V_{ext}(x) = m\omega_{ho}^2 x^2/2$ and a periodic perturbation $U_p(x,t)$. The wave function $\Phi(x,t)$ is normalized to the number N of particles in the trap. Equation (1) takes account of the correct density dependence of the ground-state energy density for the 1D Bose gas in the strong-coupling limit within a local-density approximation.

It was shown by Girardeau and Wright [14] that Eq. (1) describes approximately the dynamics of the Bose gas, although it overestimates its coherence in interference patterns at small numbers of particles. Equation (1) can be cast in the form of Landau's hydrodynamic equations for a superfluid by setting $\Phi(x,t) = \sqrt{n(x,t)}\exp[i\phi(x,t)]$. This yields

$$\partial_t n(x,t) = -\partial_x[n(x,t)v(x,t)] \quad (2)$$

and

$$m\partial_t v(x,t) = -\partial_x\left[\mu_{loc}(x,t) + \frac{1}{2}mv^2(x,t)\right], \quad (3)$$

where the velocity field is defined as $v(x,t) = (\hbar/m)\partial_x\phi(x,t)$ and the local chemical potential is given by

$$\mu_{loc}(x,t) = -\frac{\hbar^2}{2m\sqrt{n(x,t)}}\partial_x^2\sqrt{n(x,t)} + V(x,t)$$
$$+\frac{\pi^2\hbar^2}{2m}n^2(x,t). \quad (4)$$

The TFA is obtained by neglecting the first term in the right-hand side of Eq. (4). Notice that the ratio of the kinetic energy to the interaction energy is proportional to N^{-2}. The fact that in the TFA the local chemical potential scales with density as $\pi^2\hbar^2 n^2/2m$, as for a noninteracting spin-polarized Fermi gas in the local-density approximation, reflects the property that the hard-core Bose gas has the same spatial profiles as those of the Fermi gas.

The boson-fermion mapping has also been extended to time-dependent phenomena [10,14]. Therefore, using the mapping *in the inverse direction* we expect that Eq. (1) describes approximately a noninteracting Fermi gas within a local-density approach. Indeed, it is easily shown that upon

neglecting the kinetic energy term in $\mu_{loc}(x,t)$ Eqs. (2) and (3) yield the equation of motion for the density fluctuations of the Fermi gas in the hydrodynamic regime. This is given by [15]

$$m\partial_t^2 n(x,t) = \partial_x^2\Pi(x,t) + \partial_x[n(x,t)\partial_x V(x,t)], \quad (5)$$

where the momentum flux density $\Pi(x,t)$ depends locally on the particle density through the relation

$$\Pi(x,t) = \hbar^2\pi^2 n^3(x,t)/3m + mn(x,t)v^2(x,t)/2. \quad (6)$$

Equations (5) and (6) are obtained quite straightforwardly by combining Eqs. (2)–(4) in the TFA.

Having established that Eq. (1) describes in the TFA limit the dynamics of both hard-core bosons in the strong-coupling regime and noninteracting spinless fermions in the hydrodynamic regime, we turn to its equilibrium solution, which is a necessary preliminary step for obtaining the collective modes.

The ground-state density $n_0(x)$ is obtained from Eq. (3) by setting $\mu_{loc}(x) = \mu$ with $v = 0$ and $U_p = 0$. This yields the following differential equation for the equilibrium density:

$$-\frac{\hbar^2}{2m}\partial_x^2\sqrt{n_0(x)} + \frac{\pi^2\hbar^2}{2m}n_0^{5/2}(x) + [V_{ext}(x) - \mu]\sqrt{n_0(x)} = 0. \quad (7)$$

It is important to remark that Eq. (3) does not yield the exact equilibrium density profile of the gas even if one includes the kinetic energy term $(\hbar^2/2m)\partial_x^2\sqrt{n_0(x)}$. The exact profile satisfies instead the third-order differential equation [16]

$$-\frac{\hbar^2}{8m}\partial_x^3 n_0(x) - \frac{1}{2}n_0(x)\partial_x V_{ext}(x) + [V_{ext}(x) - \mu]\partial_x n_0(x)$$
$$= 0. \quad (8)$$

In the case of $N = 100$ particles an accurate comparison between the solutions of Eq. (7) (obtained by the numerical method described in Sec. IV below) and of Eq. (8) (using the results of Ref. [17]) is given in Fig. 1. It is seen that, although the overall shape of the two curves is quite similar, Eq. (7) misses the shell structure of the exact profile and has an incorrect behavior in the tails (see the insets in Fig. 1) (see also Ref. [13]).

The above comparison illustrates the limits of validity of Eq. (1). We shall see in the following that the spillout of the particle density beyond the classical radius plays a crucial role in determining the dynamics of the atomic cloud. We may also remark that, whereas Eq. (1) is constructed from an approximation for the kinetic energy density functional, the exact functional is in fact explicitly known for this system [16]. However, it involves a complicated nonlocal function of the particle density.

III. COLLECTIVE MODES IN THE THOMAS-FERMI LIMIT

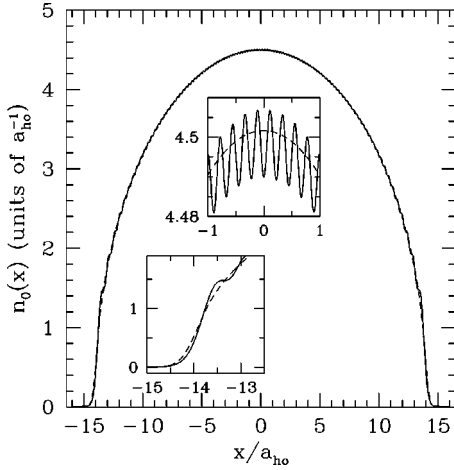The linearized equation of motion for small-amplitude density fluctuations is

FIG. 1. Equilibrium density profile for $N=100$ fermions, in units of the harmonic oscillator length $a_{ho}=\sqrt{\hbar/m\omega_{ho}}$. The exact profile (solid line) is compared with that obtained from the nonlinear Schrödinger equation (1) (dashed line). The insets show enlargements of the region around $x=0$ and of the tail region, in the same units.

$$m\partial_t^2 \delta n(x,t)=\partial_x^2 \delta\Pi(x,t)+\partial_x[\delta n(x,t)\partial_x V_{ext}(x)], \quad (9)$$

where $\delta n(x,t)=n(x,t)-n_0(x)$ and we have assumed resonance conditions, i.e., $U_p(x,t)=0$. In the homogeneous gas $V_{ext}(x)=0$ and Eq. (9) yields an acoustic dispersion relation with the propagation velocity v_F of hydrodynamic sound. It is a peculiarity of the ideal 1D Fermi gas that this coincides with the velocity of collisionless sound.

In the strict TFA limit the equilibrium density profile has finite extension, as is given by

$$n_0^{TF}(x)=\frac{\sqrt{2m}}{\pi\hbar}\,\theta(X_F^2-x^2)[\mu-V_{ext}(x)]^{1/2} \quad (10)$$

where the chemical potential $\mu=\hbar\omega_{ho}N$ is obtained from normalization of Eq. (10) to the number N of particles in the trap. We define the classical turning point as the Fermi radius $X_F=\sqrt{2N}a_{ho}$ with $a_{ho}=\sqrt{\hbar/m\omega_{ho}}$. Correspondingly, the TFA expression for the fluctuations in the momentum flux density is $\delta\Pi_{TFA}(x,t)=2\,\theta(X_F^2-x^2)[\mu-V_{ext}(x)]\delta n(x,t)$. As will be apparent from the arguments given below, the spectrum of collective excitations is obtained as a *continuum* if this expression is used in Eq. (9).

A *discrete* spectrum is instead obtained if the spillout outside the classical radius is taken into account. To do this, we adopt the approximate relation

$$\delta\Pi(x,t)\simeq 2\frac{\delta t}{\delta n}\delta n(x,t)=2[\mu-V_{ext}(x)]\delta n(x,t), \quad (11)$$

where $t(n)$ is the kinetic energy density and the second equality follows from using the Euler equation for density functional theory.

By substituting Eq. (11) into Eq. (9) and performing a Fourier transform with respect to time, we rewrite Eq. (9) as the eigenvalue equation

$$(1-z^2)\partial_z^2 \delta n(z,\omega)-3z\partial_z \delta n(z,\omega)$$
$$+[(\omega/\omega_{ho})^2-1]\delta n(z,\omega)$$
$$=0, \quad (12)$$

where $z=x/X_F$ is a rescaled position variable. It can be checked by direct substitution that for $|z|<1$ two independent solutions of this second-order differential equation are

$$\delta n_{in}^{(1)}(z,\omega)=\frac{\cos[(\omega/\omega_{ho})\arccos z]}{\sqrt{1-z^2}} \quad (13)$$

and

$$\delta n_{in}^{(2)}(z,\omega)=\frac{\sin[(\omega/\omega_{ho})\arccos z]}{\sqrt{1-z^2}} \quad (14)$$

for *any* value of the ratio ω/ω_{ho}. In the domain $|z|>1$ we instead have

$$\delta n_{out}(z,\omega)=\frac{(|z|-\sqrt{z^2-1})^{\omega/\omega_{ho}}}{\sqrt{z^2-1}}, \quad (15)$$

having imposed the condition that the density fluctuations vanish for $|z|\to\infty$. Finally, the dispersion relation and the shape of the density fluctuation modes inside the classical radius are obtained by imposing continuity of $\sqrt{|1-z^2|}\,\delta n(z,\omega)$ across the Fermi radius. This condition selects the integer values of the frequency ratio

$$\omega/\omega_{ho}=n \quad (16)$$

and the form (13) of the inner solution. This can also be written as

$$\delta n_{in}^{(1)}(z,n\omega_{ho})=\frac{T_n(z)}{\sqrt{1-z^2}} \quad (17)$$

where the functions $T_n(z)$ are Chebyshev orthogonal polynomials of the first kind [18]. The (integrable) divergence in Eq. (17) at the Fermi radius is a consequence of the linearized TFA in low dimensionality and is evidently inconsistent with the linearization of the hydrodynamic equations. We shall return on this point in the next section.

In the case $n=1$ we correctly recover from Eq. (16) the frequency of the sloshing mode, in agreement with the generalized Kohn theorem [19]. More generally, we find that the TFA spectrum coincides with the spectrum of the Fermi gas in the collisionless regime, as evaluated in Ref. [12]. Although this result for the trapped gas has been reached by an approximate and to some extent *ad hoc* argument, it will be verified immediately below by direct numerical solution of Eq. (1).

IV. NUMERICAL SIMULATION

The divergence of the density fluctuations at the classical boundary of the cloud that results from the extended TFA is incompatible with a linearization of the equations of motion.
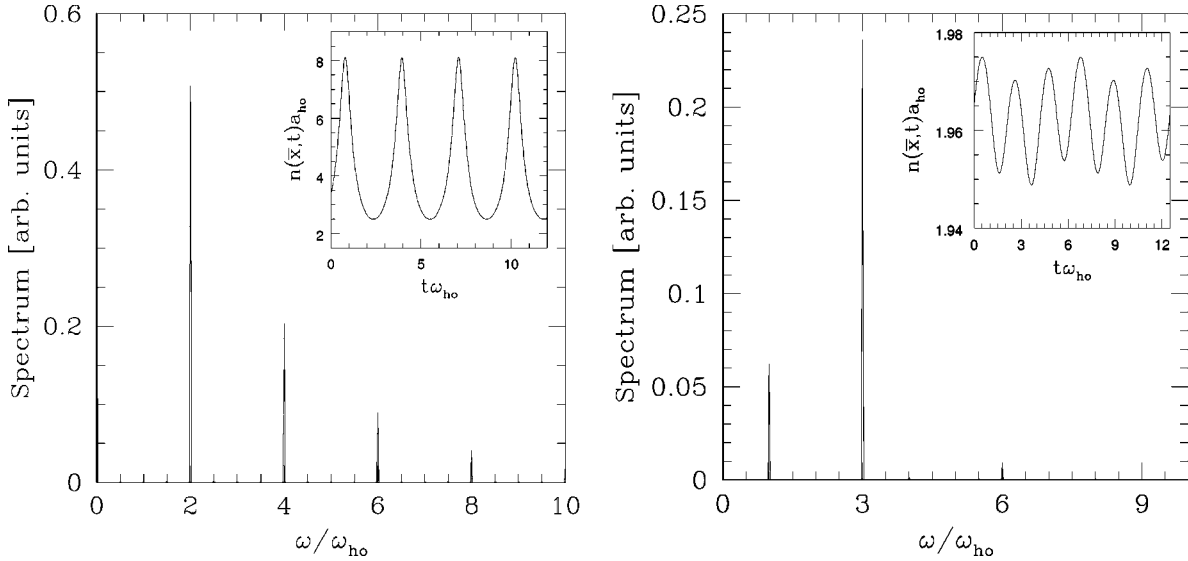
FIG. 2. Spectra of density fluctuations obtained from the numerical simulation by applying a perturbing potential of drive frequency $\omega = 2\omega_{ho}$ (left panel) and $\omega = 3\omega_{ho}$ (right panel) and of the appropriate symmetry as described in the text. The insets show the corresponding time evolution of the density profile $n(\bar{x}, t)$ (in units of a_{ho}^{-1}, with t in units of ω_{ho}^{-1}) taken at a given point $\bar{x}$ in the trap. The spectra are obtained from the Fourier transform of $n(\bar{x}, t)$, extended over several periods for a better definition of the mode frequencies.

We have therefore carried out a numerical solution of Eq. (1), which reproduces an experimental procedure employed to excite collective modes [3]. That is, we first apply a time-dependent perturbing field of given symmetry for variable amounts of time corresponding to several periods of the expected excitation, and then monitor the evolution of the cloud by recording a series of "pictures" once the perturbation is turned off. From the evolution of the density profiles we obtain the frequency and the shape of the density fluctuation modes.

The numerical simulations use an explicit time-marching algorithm [20] for propagating the state of the cloud in both imaginary and real time, yielding the ground-state profile $n_0(x)$ and the subsequent dynamical behavior $n(x, t)$. Due to the size of the nonlinear term in Eq. (1), special attention has been given to the stability of the algorithm. The perturbing potential has the form $U_p(x, t) = U_p(x)\cos(\omega_i t)$ and the drive frequency ω_i is tuned around the expected resonances. As to the spatial variation of the perturbation, we have adopted the TFA form $U_p(x) \propto \sqrt{1 - (x/X_F)^2}\, \delta n_{in}^{(1)}(x, \omega_i)$ in order to excite well defined modes. This is approximately equivalent to imposing orthogonality between the drive field and the other density fluctuations, in view of the orthogonality of the Chebyshev polynomials in the domain $|z| < 1$.

Figure 2 shows the spectra of quadrupole and hexapole collective modes for $N = 100$ particles as obtained from the Fourier transform of the time evolution of the density profile taken at a given point in the harmonic trap. The results agree with the TFA prediction that the main frequencies of these modes are $\omega = 2\ \omega_{ho}$ and $\omega = 3\ \omega_{ho}$, respectively. Nonlinearity is apparent through the presence of several other resonances in each spectrum. We have checked that the spectra of the ith moments $\langle x^i \rangle = (1/N) \int dx\, x^i n(x, t)$ are peaked at the fundamental excitation frequency of each mode. In further tests we have (i) examined the behavior of the quadrupole

mode frequency with varying N, finding only very small deviations within the error bars from the value $\omega = 2\omega_{ho}$ at low N; and (ii) used noninteger values for the driving frequency, finding again only spectral lines at integer frequencies.

Finally, in the regime of weak drive amplitude we have compared the density fluctuation profiles in Eqs. (13) and (15) with the output of the simulation. The comparison is illustrated in Fig. 3. The TFA density fluctuations, in addition to suffering from divergencies at the classical radius, do not integrate to zero for the modes with n an even integer.
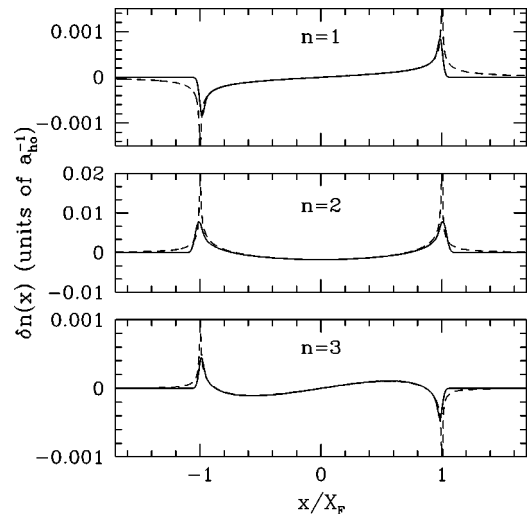

FIG. 3. Density fluctuation profiles $\delta n(x)$ for the low-lying modes (indicated by the mode numbers $n = 1$, 2, and 3 from top to bottom) at $N = 100$ particles, in units of a_{ho}^{-1} as functions of position x in units of the Thomas-Fermi radius X_F. The results from the numerical simulation (solid lines), where $\delta n(x) = n(x, \bar{t}) - n_0(x)$ and $\bar{t}$ is a given time, are compared with the analytic solutions in the Thomas-Fermi limit (dashed lines).

V. SUMMARY AND CONCLUSIONS

In summary, we have shown by analytical and numerical arguments that the hydrodynamic frequency spectrum of the 1D ideal Fermi gas under harmonic confinement is given by integer multiples of the trap frequency. This result extends to the trapped Fermi gas a property of the homogeneous ideal Fermi gas, in which the speed of sound is the same in the hydrodynamic regime as in the collisionless regime. A more accurate treatment of the collisional regime beyond the TFA may usefully be developed in the future.

A further conclusion can be drawn from the present solution of the nonlinear Schrödinger equation describing a 1D hard-core Bose gas. By virtue of the fermion-boson mapping theorem, the frequency spectrum associated with this local-density theory reproduces the exactly known spectrum of the Bose gas under harmonic confinement.

[1] M.H. Anderson, J.R. Ensher, M.R. Matthews, C.E. Wieman, and E.A. Cornell, Science **269**, 198 (1995); K.B. Davis, M.-O. Mewes, M.R. Andrews, N.J. van Druten, D.S. Durfee, D.M. Kurn, and W. Ketterle, Phys. Rev. Lett. **75**, 3969 (1995); C.C. Bradley, C.A. Sackett, J.J. Tollett, and R. Hulet, *ibid.* **75**, 1687 (1995); D.G. Fried, T.C. Killian, L. Willmann, D. Landhuis, S.C. Moss, D. Kleppner, and J. Greytak, *ibid.* **81**, 3811 (1998).

[2] B. De Marco and D.S. Jin, Science **285**, 1703 (1999); M.J. Holland, B. De Marco, and D.S. Jin, Phys. Rev. A **61**, 053610 (2000); M.-O. Mewes, G. Ferrari, F. Schreck, A. Sinatra, and C. Salomon, *ibid.* **61**, 011403(R) (2000); F. Schrek, G. Ferrari, K.L. Corwin, J. Cubizolles, L. Khaykovich, M.-O. Mewes, and C. Salomon, Phys. Rev. A **64**, 011402 (2001).

[3] D.S. Jin, J.R. Ensher, M.R. Matthews, C.E. Wieman, and E.A. Cornell, Phys. Rev. Lett. **77**, 420 (1996); M.-O. Mewes, M.R. Andrews, N.J. van Druten, D.M. Kurn, D.S. Durfee, C.G. Townsend, and W. Ketterle, *ibid.* **77**, 988 (1996); R. Onofrio, D.S. Durfee, C. Raman, M. Köhl, C.E. Kuklewicz, and W. Ketterle, *ibid.* **84**, 810 (2000).

[4] S. Stringari, Phys. Rev. Lett. **77**, 2360 (1996); M. Edwards, P.A. Ruprecht, K. Burnett, R.J. Dodd, and C.W. Clark, *ibid.* **77**, 1671 (1996).

[5] M. Amoruso, I. Meccoli, A. Minguzzi, and M.P. Tosi, Eur. Phys. J. D **7**, 441 (1999); G.M. Bruun, Phys. Rev. A **63**, 043408 (2001).

[6] B.P. Anderson and M. Kasevich, Science **282**, 1686 (1998); I. Bloch, T.W. Hänsch, and T. Esslinger, Phys. Rev. Lett. **82**, 3008 (1999); E.W. Hagley, L. Deng, M. Kozuma, J. Wen, K. Helmerson, S.L. Rolston, and W.D. Phillips, Science **283**, 1706 (1999).

[7] E. Mandonnet, A. Minguzzi, R. Dum, I. Carusotto, Y. Castin, and J. Dalibard, Eur. Phys. J. D **10**, 9 (2000).

[8] M. Olshanii, Phys. Rev. Lett. **81**, 938 (1998); *ibid.* **86**, 5413 (2001).

[9] D.S. Petrov, G.V. Shlyapnikov, and J.T.M. Walraven, Phys. Rev. Lett. **85**, 3745 (2000).

[10] M.D. Girardeau, J. Math. Phys. **1**, 516 (1960); Phys. Rev. B **139**, B500 (1965).

[11] L. Tonks, Phys. Rev. **50**, 955 (1936).

[12] P. Vignolo, A. Minguzzi, and M.P. Tosi, Phys. Rev. A **64**, 023421 (2001).

[13] E.B. Kolomeisky, T.J. Newman, J.P. Straley, and X. Qi, Phys. Rev. Lett. **85**, 1146 (2000).

[14] M.D. Girardeau and E.M. Wright, Phys. Rev. Lett. **84**, 5239 (2000).

[15] N.H. March and M.P. Tosi, Proc. R. Soc. London, Ser. A **330**, 373 (1972).

[16] N.H. March, P. Senet, and V.E. Van Doren, Phys. Lett. A **270**, 88 (2000).

[17] P. Vignolo, A. Minguzzi, and M.P. Tosi, Phys. Rev. Lett. **85**, 2850 (2000).

[18] I.S. Gradshteyn and I.M. Ryzhik, *Table of Integrals, Series and Products* (Academic, San Diego, 1980).

[19] W. Kohn, Phys. Rev. **123**, 1242 (1961); J.F. Dobson, Phys. Rev. Lett. **73**, 2244 (1994).

[20] M.M. Cerimele, M.L. Chiofalo, F. Pistella, S. Succi, and M.P. Tosi, Phys. Rev. E **62**, 1382 (2000); M.L. Chiofalo, S. Succi, and M.P. Tosi, *ibid.* **62**, 7438 (2000).